

Synchronization of Oscillators Coupled Through Narrow-Band Networks

Jonathan J. Lynch and Robert A. York, *Senior Member, IEEE*

Abstract—The ability of two coupled oscillators to synchronize depends critically on the coupling network. Previous analyses have accurately predicted the performance of quasi-optical microwave oscillator arrays for both weak and strong coupling, but have been limited to coupling networks with bandwidths considerably larger than the locking bandwidths of the oscillators. In this paper, the authors develop a method for deriving a suitable system of nonlinear differential equations describing the oscillator amplitude and phase dynamics using a generalization of Kurokawa's method. The method is applied to the case of two Van der Pol oscillators coupled through a resonant network for a wide range of coupling strengths and bandwidths. Simple approximate formulas are developed for the size of the frequency locking region as functions of the basic circuit parameters.

Index Terms—Injection locking, oscillators.

I. INTRODUCTION

IN THE authors' previous work, coupled microwave oscillators have been modeled as simple Van der Pol oscillators coupled through either a resistive network or a broad-band network that produces a constant magnitude and phase delay between the oscillators [1]. This treatment provided a satisfactory model for many applications, and the simplicity of the equations allowed one of the authors to conceive and design an electronically steerable transmitting array requiring no electronic phase shifters and only two adjustment ports [2]. In another paper, this simple theory was extended to include the effects of an arbitrary N -port broad-band coupling network described by a set of Y - or Z -parameters [3]. This analysis is useful in showing the effects of the coupling network parameters, but is limited to cases where the coupling network bandwidth is much greater than the oscillator bandwidths. The primary reason for this limitation is that the analysis relies on an approximation of the frequency dependence of the coupling network Y -parameters that is accurate only in the immediate vicinity of the frequency about which the approximation is made. The following analysis utilizes more accurate approximations and extends its applicability to the case of extremely narrow-band coupling. Using this theory, we are able to model the dynamics of oscillators coupled through many types of circuits, in particular, high- Q cavities. In this paper, we will first develop the theory and then apply it to the simple case of two Van der Pol oscillators coupled through a resonant network.

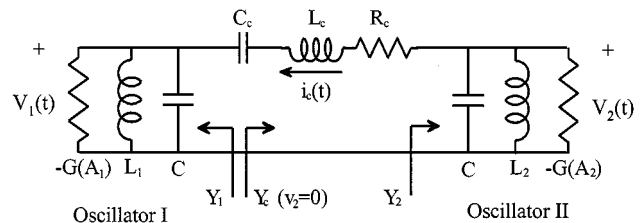


Fig. 1. Two self-sustained oscillators coupled through a resonant network.

II. DYNAMICS OF TWO OSCILLATORS COUPLED THROUGH A RESONANT CIRCUIT

For oscillators coupled through a broad-band linear network, the dynamic equations for the amplitudes and phases of each oscillator can be represented in a highly compact form for any number of oscillators and complexity of the network, as shown in [3]. If the frequency variations of the coupling network Y -parameters are significant compared to the bandwidth of the oscillators, the “broad-band” assumption breaks down and the resulting dynamic equations can be highly inaccurate. This makes sense when one considers that narrow-band coupling networks are composed of inductors and capacitors (or at least can be modeled as such) that raise the order of the overall system. One would expect that correct modeling of such systems requires additional sets of differential equations to accurately describe the dynamics of the amplitudes and phases of the coupling parameters. This is, in fact, the case, and we will show how to derive these differential equations directly from the network Y -parameters.

The theory is exemplified using a circuit composed of two parallel resonant circuits containing nonlinear negative resistance devices and coupled through a series resonant circuit, as shown in Fig. 1. The oscillators are identical, except for their resonant frequencies or tunings. All three resonant frequencies (including the coupling network) are considered arbitrary; in fact, our primary task is to determine values for them that result in frequency locking or synchronization. The frequency-domain equations can be written by inspection as follows:

$$I_c = Y_1 V_1 \quad I_c = -Y_2 V_2 \quad I_c = -Y_c (V_1 - V_2) \quad (1)$$

and explicitly show how the coupling current I_c is related to the oscillator voltages through admittance transfer functions. The oscillator transfer functions are necessarily nonlinear since a practical microwave oscillator requires a stable steady-state amplitude, and we will assume the nonlinearity is sufficiently weak so that the outputs are nearly sinusoidal. The most common model used for such applications is a linear resonant circuit containing a negative resistance or conductance whose magnitude

Manuscript received September 29, 1994.

J. J. Lynch is with HRL Research Laboratories, Malibu, CA 90265 USA.

R. A. York is with the Department of Electrical and Computer Engineering, University of California at Santa Barbara, Santa Barbara, CA 93106 USA.

Publisher Item Identifier S 0018-9480(01)01064-X.

saturates with increasing voltage amplitude. Our circuit of Fig. 1 meets these criteria if $G(A)$ is a decreasing function of amplitude. This model allows us to separate the nonlinear part of the admittance transfer function from the linear part

$$\begin{aligned} I_c &= [G_{N1}(A_1) + Y_{L1}(\omega_1)]V_1 \\ I_c &= -[G_{N2}(A_2) + Y_{L2}(\omega_2)]V_2 \\ I_c &= -Y_c(\omega_c)(V_1 - V_2) \end{aligned} \quad (2)$$

where A_1 , ω_1 are the amplitude and frequency of oscillator I, etc., and the subscripts “N” and “L” refer to the nonlinear and linear portions of the circuit. The admittance transfer functions are essentially filters that act on an “input” voltage and produce an “output” current. Since the nonlinear conductance is assumed instantaneous, the output current from this portion of the admittance is a function of the input voltage amplitude. The admittance from the linear portion of the network produces time-delayed responses so that differential equations are needed to relate input and output. For a linear transfer function $H(\omega)$ with an input expressed as $v_{in}(t) = A(t) \cos(\omega_o t + \phi(t))$, the output can be written [4] as follows:

$$v_{out}(t) = \text{Re} \left[\sum_{n=0}^{\infty} \frac{1}{n!} \frac{d^n H(\omega_o)}{d(j\omega)^n} \frac{d^n (Ae^{j\phi})}{dt^n} e^{j\omega_o t} \right]. \quad (3)$$

For a high-frequency narrow-band input signal, only the first two terms need to be retained since the derivatives of $H(\omega)$ diminish quickly with increasing n . The result is Kurokawa’s substitution [5], which is a linear approximation of the transfer function about a suitable frequency

$$\begin{aligned} v_{out}(t) &\cong \text{Re} \left[\left(H(\omega_o) + \frac{dH(\omega_o)}{d\omega} \left(\dot{\phi} - j \frac{\dot{A}}{A} \right) \right) A e^{j(\omega_o t + \phi)} \right]. \end{aligned} \quad (4)$$

Writing the output voltage in phasor notation, we have

$$A_{out} e^{j\phi_{out}} = \left(H(\omega_o) + \frac{dH(\omega_o)}{d\omega} \left(\dot{\phi} - j \frac{\dot{A}}{A} \right) \right) A e^{j\phi}. \quad (5)$$

The third term in the series (3) can be used to check the validity of the “slowly varying” assumption. Returning to (2), we must approximate the frequency-dependent parts of the admittance functions with a linear frequency dependence. The oscillator admittance function for oscillator I is

$$\begin{aligned} Y_1 &= -G_o f(A_1) + \frac{C}{j\omega_1} (\omega_{o1}^2 - \omega_1^2) \\ &\cong -G_o \left(f(A_1) + j \frac{\omega_{o1} - \omega_1}{\omega_a} \right) \end{aligned} \quad (6)$$

where $\omega_{o1} = 1/\sqrt{L_1 C}$ is the tank resonant frequency, G_o is the nonlinear device conductance at zero voltage, $f(A)$ is the saturation function for the device conductance, and $2\omega_a = G_o/C$ is the oscillator “bandwidth.” The frequency ω_1 is an arbitrary expansion frequency and the best choice is the steady-state frequency of oscillator I. If the frequency of oscillator I remains close to its “free running” or uncoupled value ω_{o1} , then the linear approximation is extremely accurate, as illustrated in Fig. 2. The admittance function for oscillator II is identical, except that ω_{o2} , ω_2 replace ω_{o1} , ω_1 . Using the first and second equations of (2) and the results of (5), we can write the dynamic

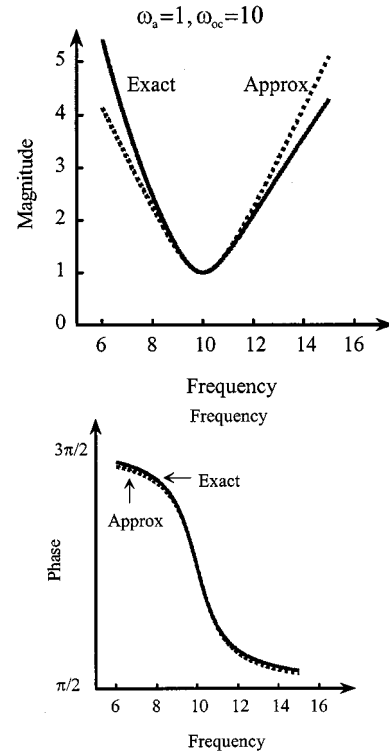


Fig. 2. Exact and approximate oscillator admittance magnitude and phase. Agreement is excellent over a broad range of frequencies.

equations for the two oscillators in terms of the coupling current. The transfer function and its derivative at frequency ω_1 are

$$Y_1(\omega_1) = -G_o \left(f(A_1) + j \frac{\omega_{o1} - \omega_1}{\omega_a} \right)$$

and

$$\frac{dY_1(\omega_1)}{d\omega_1} = j \frac{G_o}{\omega_a} \quad (7)$$

and, after inserting these expressions into (5), solving for the derivatives, and repeating for oscillator II, we find the oscillator dynamic equations are

$$\begin{aligned} \dot{A}_1 &= \omega_a f(A_1) A_1 + \omega_a I_c \cos(\theta_1 - \theta_c) \\ \dot{\theta}_1 &= \omega_{o1} - \omega_a \frac{I_c}{A_1} \sin(\theta_1 - \theta_c) \\ \dot{A}_2 &= \omega_a f(A_2) A_2 - \omega_a I_c \cos(\theta_2 - \theta_c) \\ \dot{\theta}_2 &= \omega_{o2} - \omega_a \frac{I_c}{A_2} \sin(\theta_2 - \theta_c) \end{aligned} \quad (8)$$

where we have used the instantaneous phase $\theta_i(t) = \omega_i t + \phi_i(t)$, $i = 1, 2, c$ to simplify the notation. Note that we have expressed the coupling current in terms of its slowly varying amplitude and phase as $i_c(t) = I_c(t) \cos(\omega_c t + \phi_c(t))$. The current expansion frequency ω_c is arbitrary and the equations will take on different forms depending on the choice of ω_c .

Up to this point, the analysis has been essentially the same as in [3]. We now consider the (possibly) narrow-band coupling circuit. The admittance function for the coupling network is

$$Y_c(\omega) = \frac{1}{R_c} \frac{1}{1 - j \frac{\omega_{oc}^2 - \omega^2}{2\omega\omega_{ac}}} \quad (9)$$

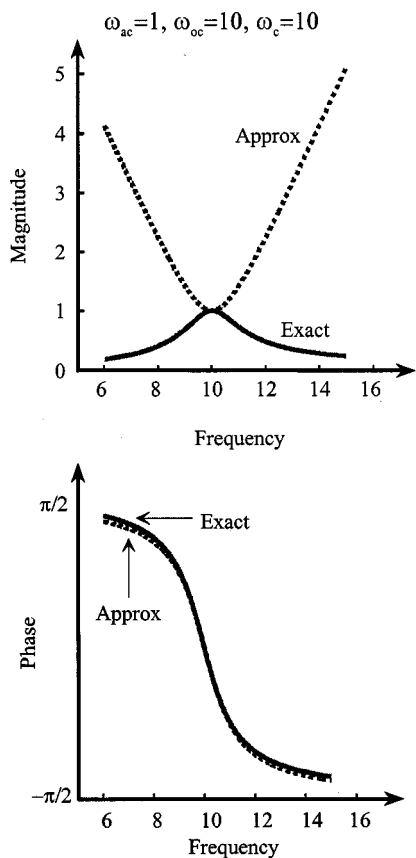


Fig. 3. Exact and approximate coupling circuit admittance magnitude and phase using linear approximation for entire transfer function. The phase is quite close, but the magnitude response is a very poor approximation.

If we were to use the broad-band assumption and expand the admittance function Y_c in a Taylor series about ω_c , as in [3], we would have the following result:

$$Y_c(\omega) \cong \frac{1}{R_c} \left[\frac{1}{1 - j \frac{\omega_{oc}^2 - \omega_c^2}{2\omega_c \omega_{ac}}} - \frac{j \frac{\omega_c}{\omega_{ac}} \frac{\omega_c^2 + \omega_{oc}^2}{2\omega_c^2} (\omega - \omega_c)}{\left(1 - j \frac{\omega_{oc}^2 - \omega_c^2}{2\omega_c \omega_{ac}}\right)^2} \right]. \quad (10)$$

Fig. 3 shows a plot of the magnitude and phase of the approximate and exact transfer functions. Although the phase response is quite close, the magnitude is a poor approximation. We would expect good agreement only very close to the expansion frequency or if the coupling network is extremely broad band. This is the “broad-band” approximation used in [3], and it is this approximation we must improve to extend the analysis to more narrow-band coupling networks.

The first step is to express the admittance function as a ratio of polynomial functions $Y_c(\omega) = N_c(\omega)/D_c(\omega)$ and write the relation between oscillator voltages and coupling currents in (2) as

$$D_c(\omega)I_c(\omega) = N_c(\omega)(V_2(\omega) - V_2(\omega)). \quad (11)$$

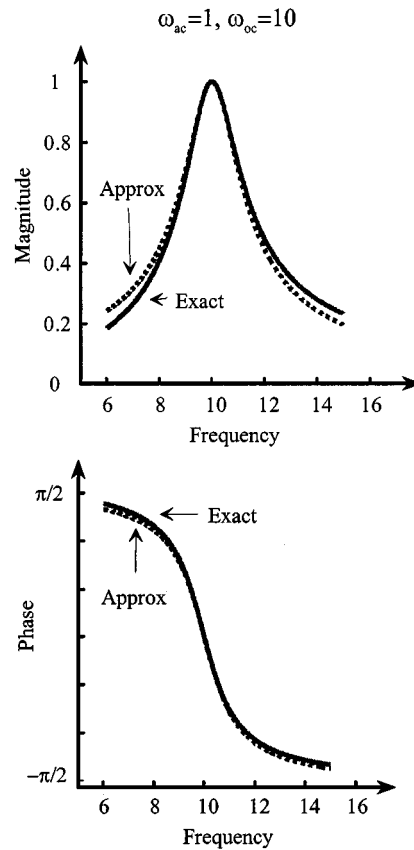


Fig. 4. More accurate approximation of coupling circuit admittance using separate linear approximations of numerator and denominator.

The transfer functions D_c and N_c operate on the current and voltage separately and we may apply Kurokawa’s substitution to each. This has the effect of linearizing the numerator and denominator of the admittance function separately and leads to a highly accurate approximation

$$Y_c(\omega) \cong \frac{1}{R_c} \frac{1}{1 - j \frac{\omega_{oc}^2 - \omega_c^2}{2\omega_c \omega_{ac}} + j \frac{\omega - \omega_c}{\omega_{ac}}} \cong \frac{1}{R_c} \frac{1}{1 - j \frac{\omega_{oc} - \omega}{\omega_{ac}}}. \quad (12)$$

The magnitude and phase response of (12) are compared to the exact response (9) in Fig. 4. Using (11) and applying Kurokawa’s substitution, we have

$$\begin{aligned} D_c(\omega_c)I_c e^{j\theta_c} + \frac{dD_c(\omega_c)}{d\omega} \left(\dot{\phi}_c - j \frac{\dot{I}_c}{I_c} \right) \\ = \frac{1}{R_c} (A_2 e^{j\theta_2} - A_1 e^{j\theta_1}) \\ \rightarrow \left[1 - j \frac{\omega_{oc} - \omega_c}{\omega_{ac}} + j \frac{1}{\omega_{ac}} \left(\dot{\phi}_c - j \frac{\dot{I}_c}{I_c} \right) \right] I_c e^{j\theta_c} \\ = \frac{1}{R_c} (A_2 e^{j\theta_2} - A_1 e^{j\theta_1}). \end{aligned} \quad (13)$$

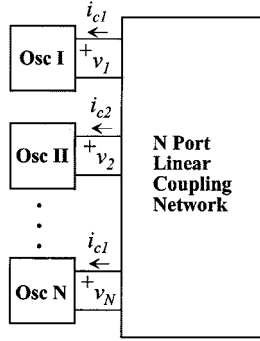


Fig. 5. N oscillators connected through an arbitrary linear coupling network.

Rearranging terms gives the dynamic equations for the amplitude and phase of the coupling current

$$\begin{aligned} \dot{I}_c &= -\omega_{ac} I_c + \frac{\omega_{ac}}{R_c} \left(V_2 \cos(\theta_2 - \theta_c) - (V_1 \cos(\theta_1 - \theta_c)) \right) \\ \dot{\theta}_c &= \omega_{oc} + \frac{\omega_{ac}}{R_c I_c} \left(V_2 \sin(\theta_2 - \theta_c) - (V_1 \sin(\theta_1 - \theta_c)) \right). \end{aligned} \quad (14)$$

Equations (8) and (14) together represent the dynamic equations for the amplitudes and phases of the oscillators and the coupling current. The order of the system matches the order of the exact system and, due to the high accuracy of the approximations, we expect the dynamics of the approximate system to give good agreement with the exact system.

III. COMPLEX SYSTEMS

The procedure outlined in the previous section can be extended to higher order systems. For N oscillators coupled through an N -port network, as shown in Fig. 5, the frequency-domain equations can be written

$$I_n = Y_n^{\text{osc}} V_n \quad I_n = \sum_{p=1}^N Y_{np}^{\text{coup}} V_p, \quad n = 1, 2, \dots, N. \quad (15)$$

Any coupling admittances with strong frequency dependence that require the denominator expansion used in the previous section should be removed from the sum and handled separately. For example, suppose that the i th and j th terms in the sum above have rapid frequency dependence. The network equations become

$$\begin{aligned} I_n &= Y_n^{\text{osc}} V_n \\ I_n &= \sum_{\substack{p=1, \\ p \neq i, j}}^N Y_{np}^{\text{coup}} V_p + I_{ni} + I_{nj} \\ D_{ni}^{\text{coup}} I_{ni} &= N_{ni}^{\text{coup}} V_i \\ D_{nj}^{\text{coup}} I_{nj} &= N_{nj}^{\text{coup}} V_j. \end{aligned} \quad (16)$$

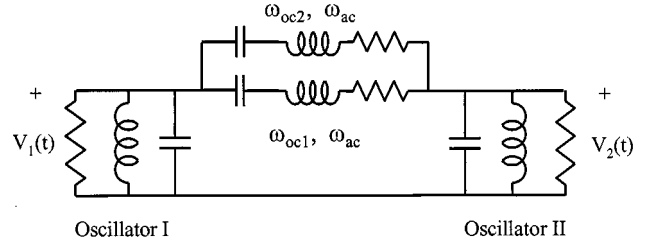


Fig. 6. Fourth-order coupling network. The overall admittance transfer function can be divided into sums of simpler functions using the partial fraction expansion technique. This method is essentially one of approximating the poles and zeros of the coupling network admittance function.

The narrow-band admittances produce additional pairs of differential equations for the associated coupling currents, which produces an approximate system of nearly the same order as the original (depending on the number of such terms that exist).

One may find that an admittance function cannot be adequately represented by a linear approximation of the numerator and denominator. For example, if, in our circuit of Fig. 1, the coupling network was composed of two second-order resonant networks, as shown in Fig. 6, the coupling admittance transfer function would be fourth order instead of second, as shown in

$$\begin{aligned} Y_c(\omega) &= \frac{2}{R_c} \left[\frac{1 - j \left(\frac{\omega_{oc1}^2 + \omega_{oc2}^2 - \omega^2}{2} \right)}{2\omega\omega_{ac}} \right] \\ &= \frac{2}{R_c} \left[\frac{1 - \frac{(\omega_{oc1}^2 - \omega)(\omega_{oc2}^2 - \omega)}{(2\omega\omega_{ac})^2} - j2 \left(\frac{\omega_{oc1}^2 + \omega_{oc2}^2 - \omega^2}{2} \right)}{2\omega\omega_{ac}} \right]. \end{aligned} \quad (17)$$

Using a partial fraction expansion expresses the admittance as the sum of two second-order functions. For this contrived example, this step is easy as follows:

$$\begin{aligned} Y_c &= \frac{1}{R_c} \left[\frac{1}{1 - j \frac{\omega_{oc1}^2 - \omega^2}{2\omega\omega_{ac}}} + \frac{1}{1 - j \frac{\omega_{oc2}^2 - \omega^2}{2\omega\omega_{ac}}} \right] \\ &= Y_{c1} + Y_{c2} \end{aligned} \quad (18)$$

and, as before, we define two coupling currents, one due to each admittance function. Once again, we are increasing the order of the system to achieve more accurate results.

IV. TWO VAN DER POL OSCILLATORS COUPLED THROUGH A RESONANT NETWORK

The above analysis techniques will be applied to the case of two Van der Pol oscillators coupled through a resonant network, as shown in Fig. 1. The dynamic equations relating the slowly

varying quantities are given in (8) and (14) and above, and repeated as follows for convenience:

$$\begin{aligned}
\dot{A}_1 &= \omega_a(1 - A_1^2)A_1 + \omega_a [A_{cx} \cos(\phi_1) + A_{cy} \sin(\phi_1)] \\
\dot{\phi}_1 &= \omega_{o1} - \omega - \omega_a \frac{1}{A_1} [A_{cx} \sin(\phi_1) - A_{cy} \cos(\phi_1)] \\
\dot{A}_2 &= \omega_a(1 - A_2^2)A_2 - \omega_a [A_{cx} \cos(\phi_2) + A_{cy} \sin(\phi_2)] \\
\dot{\phi}_2 &= \omega_{o2} - \omega + \omega_a \frac{1}{A_2} [A_{cx} \sin(\phi_2) - A_{cy} \cos(\phi_2)] \\
\dot{A}_{cx} &= -\omega_{ac}A_{cx} + (\omega - \omega_{oc})A_{cy} \\
&\quad + \omega_{ac}\lambda_o [A_2 \cos(\phi_2) - A_1 \cos(\phi_1)] \\
\dot{A}_{cy} &= -(\omega - \omega_{oc})A_{cx} - \omega_{ac}A_{cy} \\
&\quad + \omega_{ac}\lambda_o [A_2 \sin(\phi_2) - A_1 \sin(\phi_1)]
\end{aligned} \tag{19}$$

where the oscillator bandwidths are $2\omega_a = G_o/C$, the unloaded coupling circuit bandwidth is $2\omega_{ac} = R_c/L_c$, the oscillator uncoupled resonant frequencies, or tunings, are $\omega_{o1} = 1/\sqrt{L_1C}$ and $\omega_{o2} = 1/\sqrt{L_2C}$, and the coupling constant is $\lambda_o = 1/G_oR_c$. These five parameters directly affect the ability of the oscillators to lock and our task is to understand the effects of each on this ability. The coupling equations are represented in “rectangular” form rather than “polar” form using the transformation

$$\begin{aligned}
A_{cx} &= I_c \cos(\theta_c) = I_c \cos(\omega t + \phi_c) \\
A_{cy} &= I_c \sin(\theta_c) = I_c \sin(\omega t + \phi_c)
\end{aligned} \tag{20}$$

because the current amplitude can drop to zero or become negative. This occurrence does not present formal mathematical difficulties, but is avoided by using the rectangular form. Note also that we have chosen the coupling circuit “reference” frequency ω_c equal to the steady-state oscillator frequency ω to simplify the equations. The steady synchronized states are found by setting the derivatives in (19) equal to zero and solving the algebraic system for the amplitudes, phase difference $\Delta\phi = \phi_2 - \phi_1$, and the frequency ω (note that one of the oscillator phases is arbitrary due to the arbitrary time origin). The two coupling variables A_{cx} and A_{cy} can be eliminated so that the resulting system consists of four equations in four unknowns. Once a locked state is found, stability of the state can be tested by perturbing the variables of (19) and observing whether the perturbations increase or decrease in time. Perturbing the variables produces a linear system of differential equations with constant coefficients, and when the real parts of the eigenvalues of this system are all negative, the state is stable [6].

V. SYNCHRONIZED STATES

Different characteristics of the system are important in different situations. For example, the variation of the phase difference is important in the design of beam scanning systems [7]–[10], and the frequency modulation bandwidth and array settling time are important in wide-band communication systems, and these characteristics may be examined using (19). The focus of this paper, however, is on understanding how the

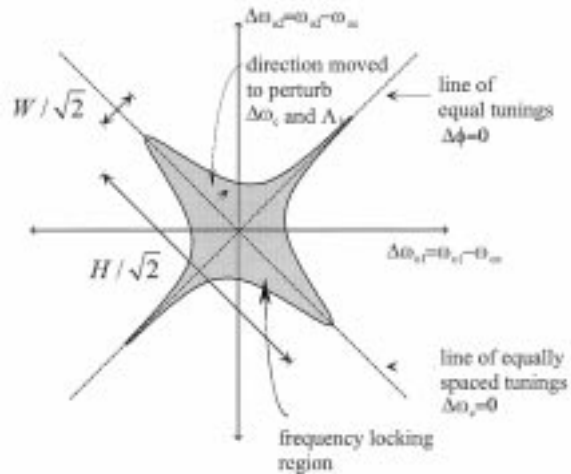


Fig. 7. Region of frequency locking in the plane of oscillator tunings with respect to the coupling circuit resonant frequency. The lines of symmetry are the lines of equal tunings $\omega_{o1} = \omega_{o2}$ and equally spaced tunings $(1/2)(\omega_{o1} + \omega_{o2}) = \omega_{oc}$. The width W is the total span of $\Delta\omega_{o1} + \Delta\omega_{o2}$ at half the maximum value of $\Delta\omega_{o2} - \Delta\omega_{o1}$. The small arrow shows the direction of the perturbation used for the Appendix.

frequency-locking ability of the oscillators depends on the coupling strength, bandwidth, and oscillator tunings for many practical combinations of each. The oscillator and coupling circuit tunings that result in frequency locking are expressed graphically in Fig. 7, where the axes are the oscillator tunings referred to the unloaded coupling circuit resonant frequency. The region enclosing the origin is where frequency locking occurs; i.e., if the oscillator tunings lie within this region, the oscillators will synchronize.¹ Our task is to determine the size and shape of this region for various values of coupling strength, coupling bandwidth, and oscillator bandwidth. In (19), we refer the oscillator tunings and the frequency ω to the coupling circuit resonant frequency using the substitutions

$$\Delta\omega_{o1} = \omega_{o1} - \omega_{oc} \quad \Delta\omega_{o2} = \omega_{o2} - \omega_{oc} \quad \Delta\omega_c = \omega - \omega_{oc}. \tag{21}$$

Setting the derivatives equal to zero gives the algebraic equations describing the locked states that, after eliminating the coupling variables A_{cx} and A_{cy} , can be written as

$$\begin{aligned}
(1 - \lambda_o \varepsilon^2 - A_1^2)A_1 &= -\lambda_o \varepsilon A_2 \cos(\Delta\phi - \Phi) \\
\Delta\omega_{o1} - \left(1 - \lambda_o \varepsilon^2 \frac{\omega_a}{\omega_{ac}}\right) \Delta\omega_c &= -\lambda_o \varepsilon \omega_a \frac{A_2}{A_1} \sin(\Delta\phi - \Phi) \\
(1 - \lambda_o \varepsilon^2 - A_2^2)A_2 &= -\lambda_o \varepsilon A_1 \cos(\Delta\phi + \Phi) \\
\Delta\omega_{o2} - \left(1 - \lambda_o \varepsilon^2 \frac{\omega_a}{\omega_{ac}}\right) \Delta\omega_c &= \lambda_o \varepsilon \omega_a \frac{A_1}{A_2} \sin(\Delta\phi + \Phi)
\end{aligned} \tag{22}$$

where

$$\varepsilon = \frac{1}{\sqrt{1 + \left(\frac{\Delta\omega_c}{\omega_{ac}}\right)^2}}$$

¹Strictly speaking, this is the region where synchronization *may* occur, depending on initial conditions. It is the region of existence of stable synchronized states.

and

$$\Phi = \tan^{-1} \left(\frac{\Delta\omega_c}{\omega_{ac}} \right)$$

are, respectively, the coupling strength scale factor and coupling phase that result from frequency-dependent attenuation and phase delay through the coupling circuit and $|\Phi| < 90^\circ$. The form of (22) is nearly identical to the form given in [3] describing frequency-independent coupling networks, except that here the coupling parameters are frequency dependent. The left-hand sides of the equations contain terms not present in the analysis of [3] that account for the loading effects of the coupling circuit on the oscillators.

The concept of coupling magnitude and phase is useful in understanding the effect of the coupling network on the ability of the oscillators to lock and is used extensively in [3]. The main result is that the tendency to lock increases with increasing coupling strength and is maximum for zero or 180° coupling phase. In fact, for $\pm 90^\circ$ of coupling phase, the ability to lock is minimized. For the present case, we can identify a frequency-dependent coupling magnitude $\lambda_o \varepsilon(\Delta\omega_c)$ and coupling phase $\Phi(\Delta\omega_c)$ and can immediately see that these quantities depend on the location of the steady-state frequency ω relative to the coupling circuit passband. If the frequency ω lies at coupling circuit resonance, i.e., $\omega = \omega_{oc} \rightarrow \Delta\omega_c = 0$, the coupling strength and phase are both optimized, and the locking tendency is strongest. As $\Delta\omega_c/\omega_{ac}$ becomes small, coupling becomes weak and the coupling phase approaches $\pm 90^\circ$, possibly causing loss of synchronization. Thus, frequency locking depends critically on the proximity of the steady-state frequency to the coupling circuit passband. The frequency is a complicated function of the circuit parameters that we must solve for using (22). In the following section, we will apply approximate methods to estimate $\Delta\omega_c$ and use this result to determine how the locking region depends on the circuit parameters.

Solutions to (22) indicate the existence of frequency-locked states, but we will briefly pause to consider these steady states from the viewpoint of linear circuit theory. As described above, the amplitudes and phases must satisfy the frequency-domain equations with Kurokawa's substitution, which essentially replaces the steady-state frequency ω with the dynamic quantity $\omega + \dot{\phi} - j(\dot{A}/A)$ for each transfer function (see [11]). In the steady state, the amplitudes A_n and phases ϕ_n of the oscillators are constant, thus, the time derivatives in Kurokawa's substitution vanish and, therefore, the steady-state system satisfies the frequency-domain transfer functions. Since the amplitudes are constant, we can replace the amplitude-dependent conductances

with constant ones with the same values without perturbing the steady-state solution. Recalling that the locked state contains only one frequency component, we can identify the state as a mode (i.e., an eigenstate) of the linear system. This modal viewpoint can be helpful in systems with very small nonlinear conductances that can, to the first approximation, be ignored. This leads to orthonormal modes and such systems are elegantly analyzed using the average potential theory [12].

VI. STABILITY OF SYNCHRONIZED STATES

A solution to (22) indicates a state exists, but the stability of the state must be ascertained by perturbing the system and observing whether the perturbations increase or decrease in time. We will perturb the steady-state values by substituting the following into (19)

$$\begin{aligned} A_i &\rightarrow A_i + \alpha_i \\ \phi_i &\rightarrow \phi_i + \delta_i \\ A_{cx} &\rightarrow A_{cx} + \alpha_{cx} \\ A_{cy} &\rightarrow A_{cy} + \alpha_{cy} \end{aligned} \quad (23)$$

and retaining only first-order terms, where A_i , ϕ_i , etc. are the steady-state values for the mode-locked state in question and α_i , δ_i , etc. are the infinitesimal perturbations. The resulting dynamic system for the perturbations, called the variational system, is shown in (24) at the bottom of this page. All expressions appearing within the matrix are the time-independent values of the frequency-locked state. As mentioned before, one steady-state oscillator phase is arbitrary, thus, we set $\phi_1 = 0$ and $\Delta\phi = \phi_2$. This implies that the above system has only five degrees of freedom and, therefore, one of the eigenvalues is zero. It is possible to reduce the set of equations since they are linearly dependent, but the coefficients of the remaining system are considerably more complicated and the simple coupling structure is obscured. Since the above matrix has constant coefficients, the system is stable when the real parts of all of the nonzero eigenvalues are negative.

We are now prepared to determine the region in the tuning plane within which stable frequency locking occurs. Equation (22), which determines the existence, and (24), which determine stability of locked states, are sufficiently complicated to require computer evaluation of exact solutions. However, for many cases, approximations can be made to reduce the complexity. In the following section, we will derive simple expressions for the values of oscillator tunings that result in stable fre-

$$\frac{d}{dt} \begin{pmatrix} \alpha_1 \\ \delta_1 \\ \alpha_2 \\ \delta_2 \\ \alpha_{cx} \\ \alpha_{cy} \end{pmatrix} = \begin{pmatrix} \omega_a(1 - 3A_1^2) & -A_1(\Delta\omega_{o1} - \Delta\omega_c) & 0 & 0 & \omega_a & 0 \\ \frac{\Delta\omega_{o1} - \Delta\omega_c}{A_1} & \omega_a(1 - A_1^2) & 0 & 0 & 0 & \frac{\omega_a}{A_1} \\ 0 & 0 & \omega_a(1 - 3A_2^2) & -A_2(\Delta\omega_{o2} - \Delta\omega_c) & -\omega_a \cos(\Delta\phi) & -\omega_a \sin(\Delta\phi) \\ 0 & 0 & \frac{\Delta\omega_{o2} - \Delta\omega_c}{A_2} & \omega_a(1 - A_2^2) & \omega_a \frac{\sin(\Delta\phi)}{A_2} & -\omega_a \frac{\cos(\Delta\phi)}{A_2} \\ -\lambda_o\omega_{ac} & 0 & \lambda_o\omega_{ac} \cos(\Delta\phi) & -\lambda_o\omega_{ac}A_2 \sin(\Delta\phi) & -\omega_{ac} & \Delta\omega_c \\ 0 & -\lambda_o\omega_{ac}A_1 & \lambda_o\omega_{ac} \sin(\Delta\phi) & \lambda_o\omega_{ac}A_2 \cos(\Delta\phi) & -\Delta\omega_c & -\omega_{ac} \end{pmatrix} \begin{pmatrix} \alpha_1 \\ \delta_1 \\ \alpha_2 \\ \delta_2 \\ \alpha_{cx} \\ \alpha_{cy} \end{pmatrix} \quad (24)$$

quency locking for various values of coupling strength and coupling bandwidth.

VII. CASES OF PRACTICAL INTEREST

In order to simplify the analysis, we will consider cases of weak, strong, wide-band, and narrow-band coupling separately and make the appropriate approximations for each case. Taking all of these results together gives us a broad understanding of the system for a wide range of parameters. In the end, we will compare our approximate expressions for the locking region dimensions to solutions obtained by computer simulation and will find good agreement in all cases.

The first difficulty we encounter is that there may be more than one solution to (22), each solution corresponding to a different mode of oscillation. In general, there will be three stable modes for the circuit considered here, one whose frequency is located near the resonance of the coupling network and the other two whose frequencies are located near each oscillator tuning. The former is the mode of practical interest and only this mode will be studied in this paper. It has the largest locking region since its frequency is closest to the coupling circuit passband, and very often it is the only mode excited. The other two modes are possible only when the oscillators are tuned well within each other's and the coupling circuit's passbands.

There are two types of tunings for which the mode of interest is relatively easy to analyze. For equal tunings, $\Delta\omega_{o1} = \Delta\omega_{o2}$, which corresponds to the diagonal line through the first and third quadrants in Fig. 7, one can show using (22) that the phase difference $\Delta\phi$ equals zero and the oscillators will always lock no matter how far away from the origin we tune. This occurs because in-phase oscillation eliminates current flow through the coupling network and since the oscillators are identically tuned they will remain in phase in the absence of coupling. However, one can see in the figure that the locking region becomes very small as we tune far away from the origin so that, practically speaking, synchronization will be lost. When the coupling circuit resonance is located exactly between the oscillator tunings, $\Delta\omega_{o1} = -\Delta\omega_{o2}$, which corresponds to the diagonal line through the second and fourth quadrants, one can show that $\Delta\omega_c = 0$, which implies maximum coupling strength, optimum coupling phase, and equal amplitudes. We will refer to this type of tuning as "equally spaced" since all three frequencies are equally spaced. The locking region is symmetric about the diagonal lines of equal and equally spaced tunings. Once we determine the locking region boundary in one quadrant, the entire region is determined. In the analysis that follows, we will consider quantities above the line of equal tunings since the phase difference is always positive in this region and this simplifies the mathematics.

Moving along the line of equally spaced tunings, the quantity $\Delta\omega_o = \Delta\omega_{o2} - \Delta\omega_{o1}$ increases and the total change in $\Delta\omega_o$ as we traverse the entire locking region we will call the "height" and denote it H (the factor of $\sqrt{2}$ in Fig. 7 is required since the measure indicated is the diagonal length). As we move away from this line perpendicularly within the locking region, we move in the direction of even tuning and vary the quantity $\overline{\Delta\omega_o} = (1/2)(\Delta\omega_{o1} + \Delta\omega_{o2})$, which is the "average" oscillator

tunings away from the coupling circuit resonance, and eventually meet the locking region edge. Twice the total change in $\overline{\Delta\omega_o}$ at half the maximum value of $\Delta\omega_o$ we will refer to as the width W , indicated in Fig. 7. Since $\Delta\omega_c = 0$ along the line of equally spaced tunings, the value of H is relatively easy to determine. However, determining W requires knowledge of the $\Delta\omega_c$ variation as we move away from this line since the ratio $\Delta\omega_c/\omega_{ac}$ has direct bearing on W .

The functional form of the phase difference for equally spaced tunings is derived from (22) by subtracting the second and fourth equations and setting $\Delta\omega_c = 0$. The result is

$$\Delta\omega_o = \Delta\omega_{o2} - \Delta\omega_{o1} = 2\lambda_o\omega_a \sin(\Delta\phi) \quad (25)$$

and we can immediately see that solutions cannot exist for $\Delta\omega_o > 2\lambda_o\omega_a$. Although we cannot easily prove it for the general case, computer simulations suggest that a necessary condition for stability is that the phase difference lie between -90° and $+90^\circ$ for any value of coupling strength or bandwidth, and we will assume that this is true. Thus, as the oscillator tunings are moved apart, but the coupling circuit resonance is maintained exactly halfway between, the phase difference increases until the locking-region boundary is encountered.

Along the line of equally spaced tunings, the amplitudes, which are equal in this case, are found from (22) as follows:

$$A^2 = 1 - \lambda_o \left(1 - \sqrt{1 - \left(\frac{\Delta\omega_o}{2\lambda_o\omega_a} \right)^2} \right). \quad (26)$$

The amplitude variation across the locking region increases with increasing coupling strength λ_o , but remains close to unity for weak coupling.

The functional dependence of $\Delta\omega_c$ can also be found by adding the second and fourth equations of (22) as follows:

$$\Delta\omega_c = \frac{\overline{\Delta\omega_o} + \frac{1}{2} \lambda_o\omega_a\epsilon^2 \left(\frac{A_2}{A_1} - \frac{A_1}{A_2} \right) \sin(\Delta\phi)}{1 - \lambda_o\epsilon^2 \frac{\omega_a}{\omega_{ac}} \left(1 - \frac{1}{2} \left(\frac{A_2}{A_1} + \frac{A_1}{A_2} \right) \cos(\Delta\phi) \right)}. \quad (27)$$

The amplitudes and the phase difference depend on the oscillator tunings through (22), and $\Delta\omega_c$ also appears implicitly in ϵ . This complexity forces us to approximate $\Delta\omega_c$ for specific cases. Since the width of the locking region depends on how fast $\Delta\omega_c$ changes as we move away from the line of equally spaced tunings, we will derive the change in $\Delta\omega_c$ for a small change in $\overline{\Delta\omega_o}$ for a fixed value of $\Delta\omega_o$. Referring to Fig. 7, we will move perpendicularly away from the diagonal as indicated. After considerable algebra (see Appendix), the approximate value for $\Delta\omega_c$ valid near the line of equally spaced tunings is

$$\Delta\omega_c \cong \frac{\overline{\Delta\omega_o}}{1 - (1 - A^2) \frac{\omega_a}{\omega_{ac}} + \frac{1}{2A^2 - 1 + \lambda_o} \frac{\Delta\omega_o^2}{4\omega_a\omega_{ac}}} \quad (28)$$

where the amplitude A is given by (26). This relation is simple enough to allow us to determine the approximate locking region width for cases of practical interest, but the approximations turn

out to be surprisingly accurate, as we will show by comparing them to computer simulations.

Whether we classify a coupling network as “narrow-band” or “broad-band” depends on the behavior of $\Delta\omega_c$ as the coupling circuit is tuned relative to the oscillators. This type of tuning is equivalent, in our analysis, to tuning in the direction perpendicular to the line of equally spaced tunings, where the spacing between the oscillators is maintained, but both are tuned relative to the coupling circuit resonance. For broad-band coupling, we would expect the steady-state frequency to be determined by the oscillator tunings and not by the coupling circuit, which implies $\Delta\omega_c \approx \overline{\Delta\omega_o} \rightarrow \omega \approx (1/2)(\omega_{o1} + \omega_{o2})$. Whereas for narrow-band coupling, we would expect the frequency to follow the coupling circuit resonance or $\Delta\omega_c \approx 0 \rightarrow \omega \approx \omega_{oc}$. These two conditions give us criteria to identify the coupling type as broad or narrow. Equation (28) tells us that for sufficiently small $\Delta\omega_o$, i.e., as $\Delta\omega_{o1}$ is tuned sufficiently close to $\Delta\omega_{o2}$, that the broad-band condition is satisfied even for small ω_{ac} , which seems to contradict our usual notion of narrow-band coupling. If the oscillators are both tuned within the unloaded coupling circuit passband, however, the steady-state frequency will always remain within this band, thus, this is essentially a “broad-band” condition. Furthermore, the effective coupling depends not on the unloaded coupling bandwidth, but on the loaded bandwidth, which involves the coupling strength and oscillator bandwidths. When the oscillator bandwidths overlap the coupling circuit bandwidth, the coupling circuit is more heavily loaded by the oscillators and, hence, the loaded Q is reduced. We must keep in mind that the definitions of broad-band and narrow-band in the following sections are somewhat arbitrary since the steady-state frequency changes in different parts of the locking region.

The division of the coupling strength and bandwidth into regions of weak/strong and narrow/broad coupling are expressed in graphical form in Fig. 8. The boundaries separating the various regions will come directly out of the analysis that follows.

A. Weak Coupling— $\lambda_o \ll 1/2$

If the resistance R_c in the coupling network of Fig. 1 becomes large, then $\lambda_o = 1/R_c G_o \ll 1/2$ and the oscillator amplitudes remain close to unity. The question immediately arises as to which terms, if any, in (28) we can neglect and under what conditions. Using the maximum value of $\Delta\omega_o$ from (25) we have, using (26), the following:

$$\Delta\omega_c|_H = \frac{\overline{\Delta\omega_o}}{1 - \lambda_o \frac{\omega_a}{\omega_{ac}} + \frac{\lambda_o^2}{1 - \lambda_o} \frac{\omega_a}{\omega_{ac}}} \quad (29)$$

and since λ_o is small, the third term in the denominator is always much less than the second and, therefore, can be neglected. At the edge of the locking region, when the second term is much less than unity, the coupling circuit is broad-band, and as unity is approached, $\Delta\omega_c$ blows up. This behavior is not what we would expect for narrow-band coupling circuits, as discussed in the previous section, and causes loss of lock fairly close to the line of equally spaced tunings. The boundary for narrow-band versus broad-band coupling can be taken as $\omega_{ac} = \lambda_o \omega_a$.

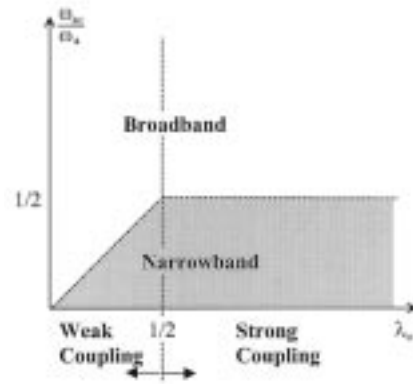


Fig. 8. Parameter diagram showing four regions of interest. Coupling strength depends only on λ_o , whereas coupling bandwidth depends on ω_a and λ_o .

1) *Broad-Band Case*— $\omega_{ac} \gg \lambda_o \omega_a$: Along the line of equally spaced tunings, one can show that stable solutions exist for all $|\Delta\phi| < \pi/2$, although proof of this will be omitted here. The height H , found from (25) and shown in Fig. 9(a), is

$$H = \Delta\omega_o|_{\max} = 2\lambda_o \omega_a. \quad (30)$$

Thus, the height of the region is proportional to the coupling strength and oscillator bandwidth. This is a well-known result that has been derived in previous papers [1].

From (28), broad-band coupling implies $\Delta\omega_c \approx \overline{\Delta\omega_o}$, which means that the steady-state frequency is exactly between the oscillator tunings and is independent of the coupling circuit resonant frequency. This can be taken as the defining characteristic of broad-band coupling. Since the amplitudes are nearly equal to unity throughout the region, the relation between the phase difference and oscillator tunings can be approximated from (22) as

$$\Delta\omega_o \cong 2\lambda_o \omega_a \frac{\omega_{ac}^2}{\omega_{ac}^2 + \Delta\omega_o^2} \sin(\Delta\phi). \quad (31)$$

Thus, the locking region boundary consists of the values of $\Delta\omega_o$ where $\Delta\phi = \pm 90^\circ$ and is plotted in Fig. 9(a). The width of the region when $\Delta\omega_o$ is half of its maximum value occurs when $\Delta\omega_c \cong \overline{\Delta\omega_o} = \omega_{ac}$, as seen from (31). Including the second term in the denominator of (28) for $\Delta\omega_o$ gives a more accurate result for the width

$$W = 2 \overline{\Delta\omega_o}|_{\Delta\omega_o=(1/2)H} \cong 2\omega_{ac} - 2 \left(1 - \frac{\sqrt{3}}{2}\right) \lambda_o \omega_a. \quad (32)$$

The case of a resistive coupling circuit can be found by letting the coupling circuit bandwidth approach infinity in (30) and (32). The result is an infinite locking region that follows the line of equal oscillator tunings, as we expect from physical considerations.

2) *Narrow-Band Case*— $\omega_{ac} \ll \lambda_o \omega_a$: We now consider small coupling circuit bandwidths. The quantity $\Delta\omega_c$ near the line of equally spaced tunings is found from (28) to be

$$\Delta\omega_c \cong \frac{\overline{\Delta\omega_o}}{1 - \frac{\lambda_o \omega_a}{\omega_{ac}} \left(1 - \sqrt{1 - \left(\frac{\Delta\omega_o}{2\lambda_o \omega_a}\right)^2}\right)}. \quad (33)$$

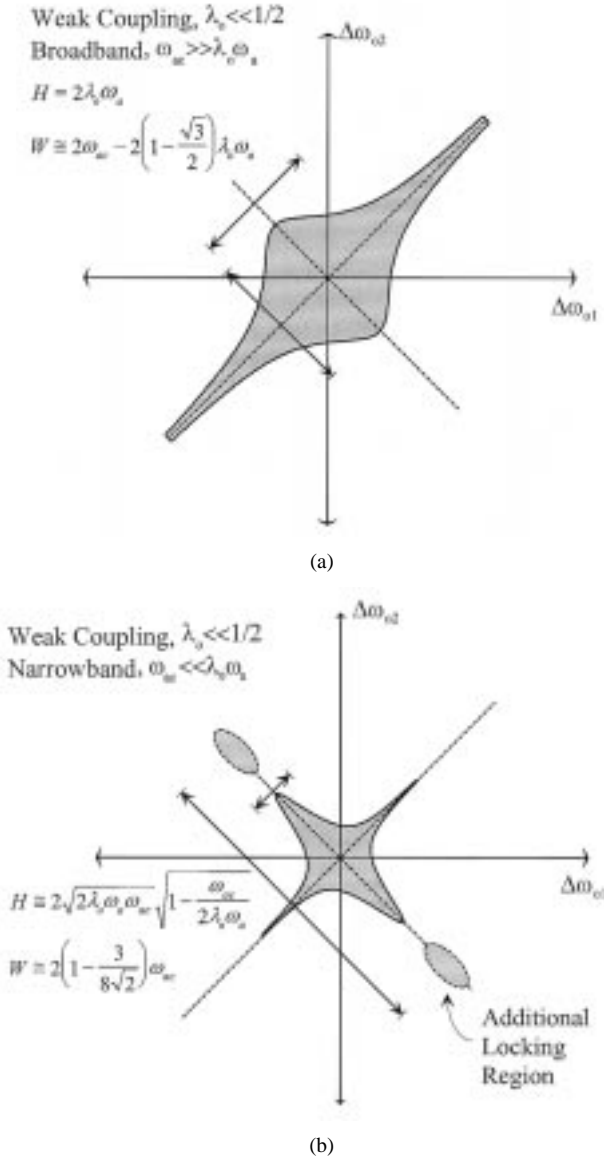


Fig. 9. Dimensions of the locking region for weakly coupled oscillators. (a) Case of broad-band coupling has a fairly wide locking region that is bounded by the phase requirement $|\Delta\phi| < \pi/2$. (b) Narrow-band case is quite thin and is bounded by loss of stability due to high sensitivity of the steady-state frequency with respect to tuning variations. The additional locking regions appear for values of λ_o near, but below, unity.

Near the center of the locking region, which is for small $\Delta\omega_o$, $\Delta\omega_c \approx \overline{\Delta\omega_o}$, and we see the same behavior as in the previous case. However, as $\Delta\omega_o$ increases, the denominator in (33) decreases, and $\Delta\omega_c$ becomes much more sensitive to tuning variations. Computer simulations show that the value of $\Delta\omega_o$ which causes the denominator to vanish is (approximately) a stability boundary, and for values of $\Delta\omega_o$, for which $\Delta\omega_c$ is negative, the system is not stable. The stability boundary and, therefore, the height of the locking region, is found by setting the denominator of (33) equal to zero

$$H = \Delta\omega_o|_{\max} \cong 2\sqrt{2\lambda_o \omega_a \omega_{ac}} \sqrt{1 - \frac{\omega_{ac}}{2\lambda_o \omega_a}}. \quad (34)$$

For coupling bandwidths above $2\lambda_o \omega_a$ this stability boundary does not exist. Below this threshold, we must also meet the gen-

eral existence criterion that $\Delta\omega_o < 2\lambda_o \omega_a$. Using these two criteria together, we find that this new stability boundary exists only for $\omega_{ac} < \lambda_o \omega_a$ and above this value of coupling bandwidth the general existence criterion applies. Assuming the former condition applies, the stability region is found, at least approximately, using

$$\Delta\omega_o \cong 2\lambda_o \omega_a \frac{\omega_{ac}^2}{\omega_{ac}^2 + \Delta\omega_c^2} \sin(\Delta\phi) \quad (35)$$

with $\Delta\omega_c$ given in (33). To find the width, we find $2\overline{\Delta\omega_o}|_{\Delta\omega_o=(1/2)H}$ which, as for the previous case, occurs at $\Delta\omega_c = \omega_{ac}$. Solving for the width gives

$$W = 2\overline{\Delta\omega_o}|_{\Delta\omega_o=(1/2)H} \cong 2\left(1 - \frac{3}{8\sqrt{2}}\right)\omega_{ac}. \quad (36)$$

Fig. 9(b) shows the approximate shape of the locking region for weak- and narrow-coupling bandwidth. The region is much thinner near the edge of the odd tuning boundary due to the increased sensitivity of $\Delta\omega_c$ to changes in $\overline{\Delta\omega_o}$ near this boundary.

If we include the third term in the denominator of (28) we find that, for values of λ_o close to, but less than unity, the denominator becomes zero a second time, and for values of $\Delta\omega_o$ greater than this critical value, the locked states are stable once again. Thus, two new locking regions appear and are disconnected from the main region [they are shown as dotted regions in Fig. 9(b)]. In this analysis, however, we will limit ourselves to small coupling parameters for which case these additional stability regions do not exist.

B. Strong Coupling— $\lambda_o \gg 1/2$

As the coupling strength λ_o is increased, the amplitudes decrease considerably as we traverse the locking region in the direction of equally spaced tunings. The physical reason for this is that, as the coupling resistor R_c is reduced, the power dissipated in it increases. The oscillator conductances must make up this power loss by becoming more negative, which is achieved by amplitude reduction. However, power dissipation in the coupling network requires a phase difference to exist between the oscillators, and this phase difference increases as we traverse the locking region. If either of the amplitudes drops too far below unity, the system becomes unstable and locking is lost. It is difficult to determine exactly when this occurs, but we can find the approximate amplitude boundary from the variational system (24).

The variational system consists of three second-order subsystems, the three diagonal blocks, and are coupled through the off diagonal blocks. If no coupling existed, then stability of the system would be insured if each of the three subsystems were stable. The coupling circuit is always stable since it contains some nonzero positive resistance, but the subcircuits representing the oscillators will become unstable if either amplitude drops excessively since low amplitudes imply net negative resistance. One can show that the matrix of coefficients of each oscillator subcircuit has a positive determinant along the line of equal tunings when the coupling coefficient λ_o is greater than unity. This implies that stability is determined by the trace of the matrix. Applying this criterion to each diagonal submatrix

in the variational system gives conditions for stability in the uncoupled case, but which we assume hold approximately in the general case

$$A_1 \text{ and } A_2 > \frac{1}{\sqrt{2}}. \quad (37)$$

This means that if either amplitude drops below $1/\sqrt{2}$, the system will become unstable. This approximate stability condition is surprisingly accurate for most values of coupling strength and bandwidth, and becomes inaccurate only when these parameters both become quite large. Even in this case, however, the dimensions of the locking region given below are fairly accurate.

For strongly coupled oscillators, the boundaries of the locking region can be approximated as the locus of points where either oscillator amplitude is $1/\sqrt{2}$. Along the line of equally spaced tunings, the value of $\Delta\omega_o$ that causes the amplitudes to assume this value can be found from (26) and is

$$H = \Delta\omega_o|_{\max} = 2\sqrt{\lambda_o}\omega_a \sqrt{1 - \frac{1}{4\lambda_o}}, \quad \text{for } \lambda_o < \frac{1}{2}. \quad (38)$$

One important consequence is that, for a coupling strength $\lambda_o = 1/2$, the locking-region height is maximized while still allowing the phase difference $\Delta\phi$ to vary 180° over the locking region. This is important for beam-scanning systems where the designer wishes to maximize the total phase variation and the locking range simultaneously.

If the coupling strength is sufficiently strong, the width of the region will also be determined by the amplitude criterion of (37). To estimate the rate of decrease of the amplitude away from the line of equally spaced tunings, we resort to a perturbation analysis, not derived here for the sake of brevity. The results show that if we move from this line in the direction of increasing $\overline{\Delta\omega_o}$, that the amplitude of oscillator I will diminish according to

$$A_1 \cong A \left(1 - \frac{\Delta\omega_o \Delta\omega_c}{4\omega_a \omega_{ac} (\lambda_o - 1 + 2A^2)} \right) \quad (39)$$

where A is given by (26). We will assume strong coupling, i.e., $\lambda_o \gg 2A^2 - 1$, and simplify the denominator. To find the width of the locking region, we will evaluate the amplitude at $\Delta\omega_o = (1/2)\Delta\omega_o|_{\max}$ and find the value of $\overline{\Delta\omega_o}$ that gives $A = 1/\sqrt{2}$. First, however, we must determine $\Delta\omega_c$.

Using (26) for the amplitude for odd tunings and noting that for large coupling strengths we can expand the square root, $\Delta\omega_c$ from (28) is approximately

$$\Delta\omega_c \cong \frac{\overline{\Delta\omega_o}}{1 + \frac{\overline{\Delta\omega_o}^2}{8\lambda_o \omega_a \omega_{ac}}}. \quad (40)$$

This shows that for $\overline{\Delta\omega_o} \ll 2\sqrt{2\lambda_o \omega_a \omega_{ac}}$, the steady-state frequency remains halfway between the two oscillators, as in the case of weak broad-band coupling, but for $\overline{\Delta\omega_o} \gg 2\sqrt{2\lambda_o \omega_a \omega_{ac}}$, the steady-state frequency follows

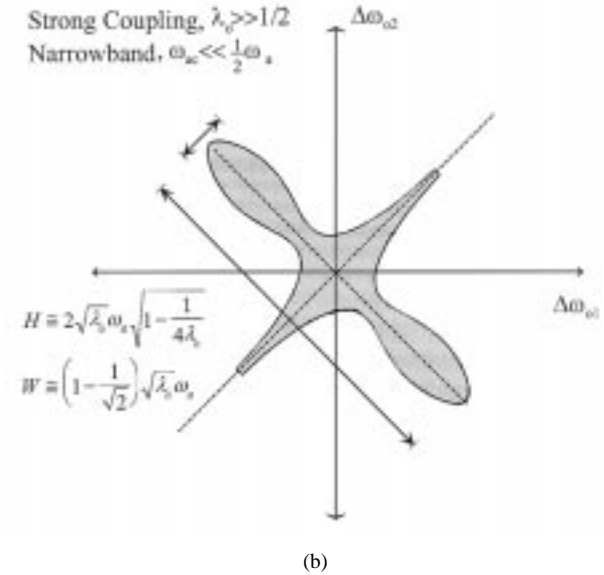
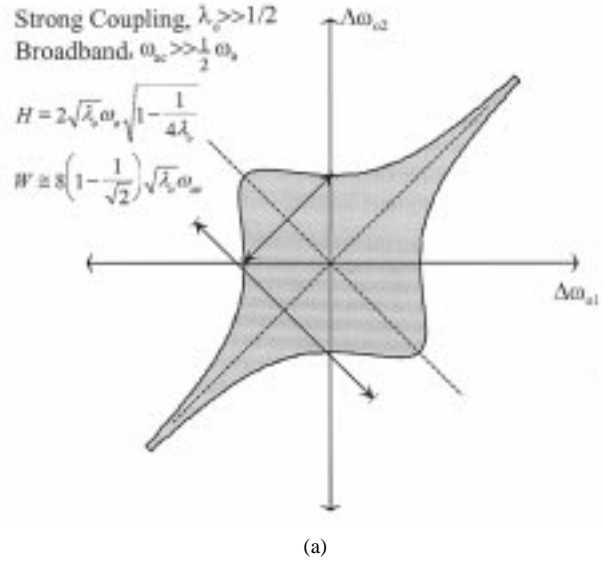


Fig. 10. Dimensions of the locking region for strongly coupled oscillators. (a) For broad-band coupling, the region is large, but increases as $\sqrt{\lambda_o}$. (b) Narrow-band case shows large region width as oscillator tunings are moved apart, but remains narrow when oscillators are tuned within the coupling circuit passband.

the resonant frequency of the coupling network. Using the above result at the maximum value of $\Delta\omega_o$ given by (38), and assuming $\lambda_o \gg 1$, we can say that the boundary for weak versus narrow-band coupling is at $\omega_{ac} \cong (1/2)\omega_a$.

1) *Broad-Band Case*— $\omega_{ac} \gg (1/2)\omega_a$: In this section, we will assume that $\omega_{ac} \gg (1/2)\omega_a$ so that $\Delta\omega_c \approx \overline{\Delta\omega_o}$. Using this result in (39) for the amplitude of oscillator I and setting the amplitude to $1/\sqrt{2}$, we find that the width of the locking region is

$$W \cong 8 \left(1 - \frac{1}{\sqrt{2}} \right) \sqrt{\lambda_o} \omega_{ac}. \quad (41)$$

The locking region for this case, shown in Fig. 10(a), looks similar to the case of weak and broad-band coupling, but the height grows more slowly with increasing coupling strength λ_o and the width is no longer constant with λ_o .

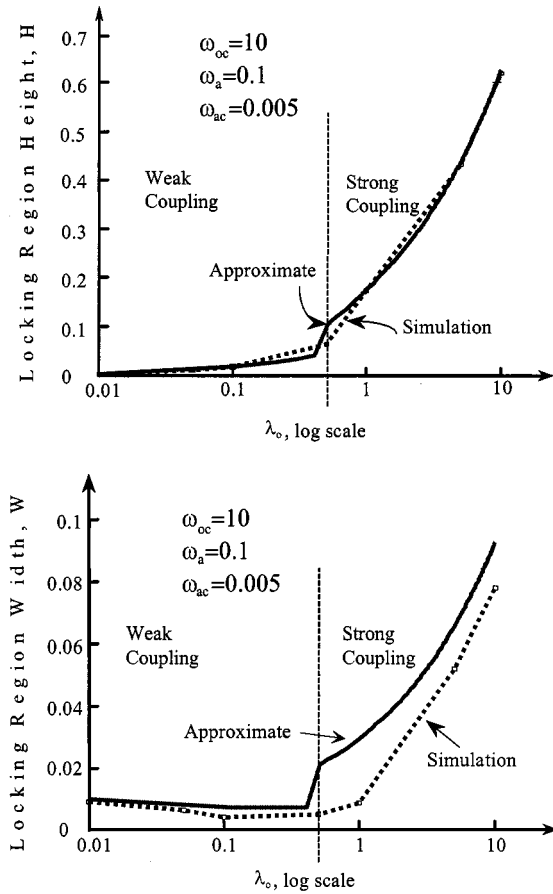


Fig. 11. Comparison of approximate formulas to computer simulations for “high”- Q coupling circuit.

2) *Narrow-Band Case*— $\omega_{ac} \ll (1/2)\omega_a$: We now have $\Delta\omega_c \approx (8\lambda_o\omega_a\omega_{ac}/\Delta\omega_o^2) \Delta\omega_o$ and using this result in (39) and setting the amplitude to $1/\sqrt{2}$, the width of the locking region is

$$W \cong \left(1 - \frac{1}{\sqrt{2}}\right) \sqrt{\lambda_o\omega_a}. \quad (42)$$

The locking region for this case is shown in Fig. 10(b), where we can see that the region gets slightly wider as we move along the line of equally spaced tunings. The reason for this behavior is that as the oscillators are tuned far apart, they influence the steady-state frequency less. Thus, the frequency can follow the coupling circuit bandwidth and strong coupling is maintained over a wide range.

VIII. COMPUTER SIMULATIONS

To verify the accuracy of the above expressions for the height and width of the locking region, MathCAD was used to obtain solutions to (22) and to compute the eigenvalues of the variational system (24) for various circuit parameters. In addition, the nonlinear differential equations (19) were also numerically integrated to verify that the steady states and eigenvalues for a particular set of parameters were correct. The coupling-circuit resonant frequency and oscillator bandwidths were kept constant at $\omega_{oc} = 10$ and $\omega_a = 0.1$. The height H and width W

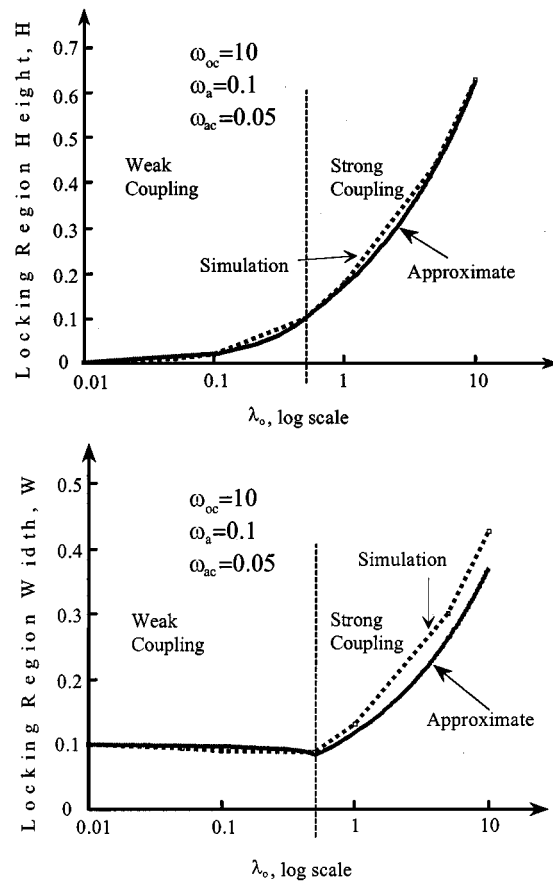


Fig. 12. Comparison of approximate formulas to computer simulations for “moderate”- Q coupling circuit.

were computed for three different values of coupling bandwidth, $\omega_{ac} = 0.005, 0.05, 0.5$ as functions of the coupling strength λ_o , and the simulation results and the results calculated from the approximate expressions are shown in Figs. 11–13.

IX. CONCLUSION

The theory developed in this paper allows one to derive a nonlinear system of differential equations for oscillators coupled through frequency-dependent networks, and shows explicitly the approximations involved in applying Kurokawa’s substitution. The theory shows the limitations of a previous analysis by the authors for broad-band coupling networks and then applies the theory to the case of two oscillators coupled through a frequency-dependent network. Simple approximate formulas for the dimensions of the locking region are derived and plotted against values determined by computer simulation. The analysis suggests specific boundaries that separate the strong/weak and narrow-band/broad-band coupling regions. An important case of practical interest is when two oscillators are coupled through a high- Q cavity. For weak coupling, the analysis shows that the locking region is quite small; the region width is on the order of the unloaded bandwidth of the coupling circuit. For strong coupling, oscillation near the resonant frequency of the cavity occurs primarily when the cavity resonance is located between the two oscillator tunings and increases as the oscillators are

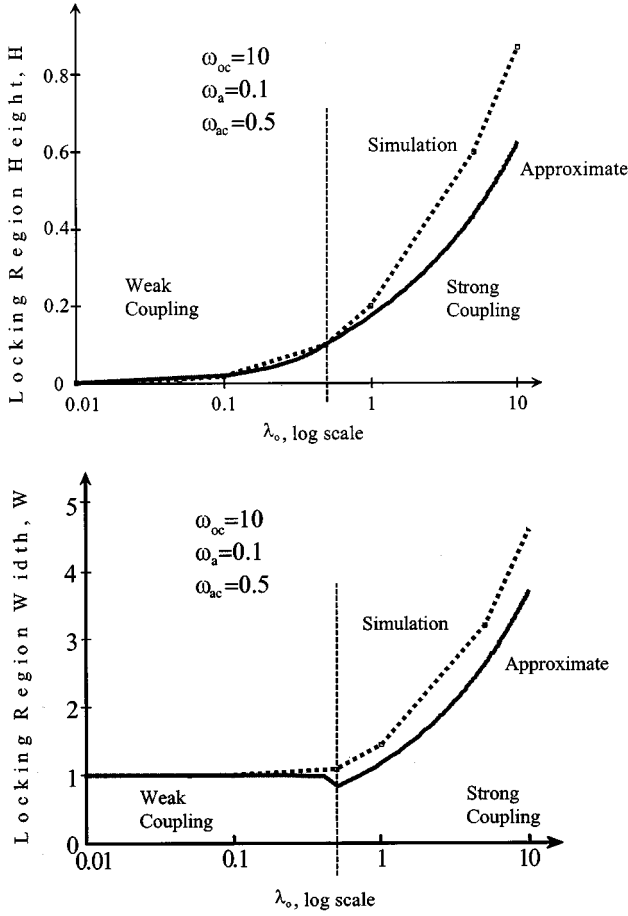


Fig. 13. Comparison of approximate formulas to computer simulations for "low"- Q coupling circuit.

tuned apart from one another. For this case, the phase difference between the oscillators remains near 0° and loss of synchronization is due to large amplitude variations.

APPENDIX

DERIVATION OF AMPLITUDES AND $\Delta\omega_c$ NEAR LINE OF EQUALLY SPACED FREQUENCIES

In this section, we derive approximate expressions for $\Delta\omega_c$ and the amplitudes A_1 and A_2 that are valid near the line of equally spaced tunings as we tune perpendicularly away from that line, as indicated by the small arrow in Fig. 7. The first and third equations of (22) relate the oscillator amplitudes to various quantities and are repeated as follows with the coupling phase expanded:

$$\begin{aligned} (1 - \lambda_o \varepsilon^2 - A_1^2) A_1 &= -\lambda_o \varepsilon^2 A_2 \left(\cos(\Delta\phi) + \frac{\Delta\omega_c}{\omega_{ac}} \sin(\Delta\phi) \right) \\ (1 - \lambda_o \varepsilon^2 - A_2^2) A_2 &= -\lambda_o \varepsilon A_1 \left(\cos(\Delta\phi) - \frac{\Delta\omega_c}{\omega_{ac}} \sin(\Delta\phi) \right). \end{aligned} \quad (43)$$

Subtracting the second fourth equations of (22), we arrive at an expression for the difference between oscillator tunings

$$\begin{aligned} \Delta\omega_o &= \Delta\omega_{o2} - \Delta\omega_{o1} \\ &= \lambda_o \varepsilon^2 \omega_a \left[\left(\frac{A_2}{A_1} + \frac{A_1}{A_2} \right) \sin(\Delta\phi) \right. \\ &\quad \left. - \frac{\Delta\omega_c}{\omega_{ac}} \left(\frac{A_2}{A_1} - \frac{A_1}{A_2} \right) \cos(\Delta\phi) \right] \end{aligned} \quad (44)$$

and adding them gives an expression for $\Delta\omega_c$

$$\begin{aligned} \Delta\omega_c &= \overline{\Delta\omega_o} + \lambda_o \varepsilon^2 \omega_a \left[\frac{\Delta\omega_c}{\omega_{ac}} + \frac{1}{2} \left(\frac{A_2}{A_1} - \frac{A_1}{A_2} \right) \sin(\Delta\phi) \right. \\ &\quad \left. - \frac{1}{2} \frac{\Delta\omega_c}{\omega_{ac}} \left(\frac{A_2}{A_1} + \frac{A_1}{A_2} \right) \cos(\Delta\phi) \right]. \end{aligned} \quad (45)$$

As we vary $\overline{\Delta\omega_o}$ an infinitesimal amount $d\overline{\Delta\omega_o}$ away from zero, many of the quantities in the above equations will change. For example, $\Delta\omega_c$ is nominally zero (this can be taken as the definition of the mode of interest), but after this perturbation, it will have a nonzero value. The quantity ε , however, depends on the square of $\Delta\omega_c$ [see (22)] thus, to the first order, ε will remain unity.

The equations are perturbed by implicit differentiation and any unperturbed terms will be evaluated on the line $\overline{\Delta\omega_o} = 0$ and, as a result, some may vanish. Along this line, (43)–(45) take on particularly simple forms, and result in the amplitude expression of (26) and the following relations for the phase difference:

$$\begin{aligned} \sin(\Delta\phi) &= \frac{\Delta\omega_o}{2\lambda_o \omega_a} \\ \cos(\Delta\phi) &= 1 - \frac{1}{\lambda_o} (1 - A^2). \end{aligned} \quad (46)$$

These relations help simplify the form of the mathematics that follows.

Implicitly differentiating the amplitude, (43) gives

$$\begin{aligned} (1 - \lambda_o - 3A^2) dA_1 &= -\lambda_o \left[dA_2 \cos(\Delta\phi) - A \left(d\Delta\phi - \frac{d\Delta\omega_c}{\omega_{ac}} \right) \sin(\Delta\phi) \right] \\ (1 - \lambda_o - 3A^2) dA_2 &= -\lambda_o \left[dA_1 \cos(\Delta\phi) - A \left(d\Delta\phi + \frac{d\Delta\omega_c}{\omega_{ac}} \right) \sin(\Delta\phi) \right] \end{aligned} \quad (47)$$

where the unperturbed quantities have been evaluated along $\overline{\Delta\omega_o} = 0$. Adding and subtracting these equations and using the relations (46) gives

$$\begin{aligned} dA_2 + dA_1 &= -\frac{\Delta\omega_o}{2A} d\Delta\phi \\ dA_2 - dA_1 &= -\frac{A}{2A^2 + \lambda_o - 1} \frac{\Delta\omega_o d\Delta\omega_c}{2\omega_a \omega_{ac}}. \end{aligned} \quad (48)$$

Applying the same analysis technique to (44), which we maintain at zero, gives

$$\begin{aligned} d\Delta\omega_o &= 0 \\ &= \lambda_o\omega_a \left[d \left(\frac{A_2}{A_1} + \frac{A_1}{A_2} \right) \sin(\Delta\phi) + 2 \cos(\Delta\phi) d\Delta\phi \right] \\ &= \lambda_o\omega_a \left[\frac{2}{A} (dA_1 + dA_2) \sin(\Delta\phi) + 2 \cos(\Delta\phi) d\Delta\phi \right]. \end{aligned} \quad (49)$$

Using the first of (48), the above expression becomes

$$\left(\frac{2}{A} \sin(\Delta\phi) - \frac{2A}{\Delta\omega_o} \cos(\Delta\phi) \right) (dA_1 + dA_2) = 0. \quad (50)$$

The first parenthetic quantity is not generally zero, thus, we must have $dA_1 + dA_2 = 0$ and, from (48), it follows that $d\Delta\phi = 0$. Using these results with the second equation of (48), we can find the approximate expression for the amplitude of oscillator II (which is the lesser), valid for small $\Delta\omega_c$, stated in (39) as follows:

$$A_2 \cong A \left(1 - \frac{1}{2A^2 + \lambda_o - 1} \frac{\Delta\omega_o \Delta\omega_c}{4\omega_a \omega_{ac}} \right). \quad (51)$$

The remaining task is to find an approximate expression for $\Delta\omega_c$. Implicitly differentiating (45) and using the relations (46) and those resulting from (50), we find

$$\begin{aligned} d\Delta\omega_c &\left[1 - \lambda_o \frac{\omega_a}{\omega_{ac}} (1 - \cos(\Delta\phi)) \right] \\ &= d\overline{\Delta\omega_o} + \frac{1}{2} \lambda_o \omega_a d \left(\frac{A_2}{A_1} - \frac{A_1}{A_2} \right) \sin(\Delta\phi) \\ &= d\overline{\Delta\omega_o} - \lambda_o \omega_a \sin(\Delta\phi) \frac{1}{2A^2 + \lambda_o - 1} \frac{\Delta\omega_o d\Delta\omega_c}{2\omega_a \omega_{ac}} \\ &= d\overline{\Delta\omega_o} - \frac{1}{2A^2 + \lambda_o - 1} \frac{\Delta\omega_o^2}{4\omega_a \omega_{ac}} d\Delta\omega_c \end{aligned} \quad (52)$$

which, after rearrangement, gives (28) valid for small $\overline{\Delta\omega_o}$ and $\Delta\omega_c$ as follows:

$$\Delta\omega_c \cong \frac{\overline{\Delta\omega_o}}{1 - (1 - A^2) \frac{\omega_a}{\omega_{ac}} + \frac{1}{2A^2 - 1 + \lambda_o} \frac{\Delta\omega_o^2}{4\omega_a \omega_{ac}}}. \quad (53)$$

REFERENCES

- [1] R. A. York, "Nonlinear analysis of phase relationships in quasi-optical oscillator arrays," *IEEE Trans. Microwave Theory Tech.*, vol. 41, pp. 1799–1809, Oct. 1993.

- [2] P. Liao and R. A. York, "A new phase-shifterless beam-scanning technique using arrays of coupled oscillators," *IEEE Trans. Microwave Theory Tech.*, vol. 41, pp. 1810–1815, Oct. 1991.
- [3] R. A. York, P. Liao, and J. J. Lynch, "Oscillator array dynamics with broad-band N -port coupling networks," *IEEE Trans. Microwave Theory Tech.*, vol. 42, pp. 2040–2045, Nov. 1994.
- [4] J. J. Lynch, "Analysis and design of arrays of coupled microwave oscillators," Ph.D. dissertation, Dept. Elect. Comput. Eng., Univ. California, Santa Barbara, CA, 1996.
- [5] K. Kurokawa, "Injection locking of solid state microwave oscillators," *Proc. IEEE*, vol. 61, pp. 1386–1409, Oct. 1973.
- [6] G. Strang, *Linear Algebra and Its Applications*. New York: Academic, 1980.
- [7] J. J. Lynch, H. C. Chang, and R. A. York, "Coupled-oscillator arrays and scanning techniques," in *Active and Quasi-Optical Arrays for Solid-State Power Combining*, R. York and Z. Popović, Eds. New York: Wiley, 1997, ch. 4.
- [8] J. Lin, S. T. Chew, and T. Itoh, "A unilateral injection-locking type active phased array for beam scanning," in *IEEE MTT-S Int. Microwave Symp. Dig.*, San Diego, June 1994, pp. 1231–1234.
- [9] R. A. York and T. Itoh, "Injection- and phase-locking techniques for beam control," *IEEE Trans. Microwave Theory Tech.*, vol. 46, pp. 1920–1929, Nov. 1998.
- [10] P. S. Hall, I. L. Morrow, P. M. Haskins, and J. S. Dabele, "Phase control in injection locked microstrip active antennas," in *IEEE MTT-S Int. Microwave Symp. Dig.*, San Diego, CA, June 1994, pp. 1227–1230.
- [11] K. Kurokawa, "Injection-locking of solid state microwave oscillators," *Proc. IEEE*, vol. 61, pp. 1386–1409, Oct. 1973.
- [12] M. Kuramitsu and F. Takase, "Analytical method for multimode oscillators using the averaged potential," *Elect. Commun. Japan*, vol. 66-A, no. 4, 1983.

Jonathan J. Lynch received the B.S.E.E., M.S.E.E., and Ph.D. degrees from the University of California at Santa Barbara, in 1987, 1992, and 1995, respectively.

Since 1995, he has been with HRL Research Laboratories, Malibu, CA, where he heads the Microwave Technologies group within the Microelectronics Laboratory. His research areas include antenna development for commercial radar and communication systems, polarization conversion structures, tunable filter technologies, and RF sensors for automotive applications.



Robert A. York (S'85–M'89–SM'99) received the B.S. degree in electrical engineering from the University of New Hampshire, Durham, in 1987, and the M.S. and Ph.D. degrees in electrical engineering from Cornell University, Ithaca, NY, in 1989 and 1991, respectively.

He is currently an Associate Professor of electrical and computer engineering at the University of California at Santa Barbara (UCSB), where his group is currently involved with the design and fabrication of novel microwave and millimeter-wave circuits, microwave photonics, high-power microwave and millimeter-wave modules using spatial combining and wide-bandgap semiconductor devices, and application of ferroelectric materials to microwave and millimeter-wave circuits and systems.

Dr. York was the recipient of the 1993 Army Research Office Young Investigator Award and the 1996 Office of Naval Research Young Investigator Award.